



Research Article

A THEORETICAL PERFORMANCE INVESTIGATION OF IRREVERSIBLE INTERNAL COMBUSTION ENGINE NAMED AS DUAL-MILLER CYCLE

Yasin UST*¹, Ibrahim OZSARI², Feyyaz ARSLAN³, Aykut SAFA⁴

¹Dept. of Naval Architecture and Marine Engineering, Yildiz Technical University, Besiktas, ISTANBUL; ORCID: 0000-0002-1678-1038

²Dept. of Naval Architecture and Marine Engineering, Yildiz Technical University, Besiktas, ISTANBUL; ORCID: 0000-0003-4543-9167

³Dept. of Naval Architecture and Marine Engineering, Yildiz Technical University, Besiktas, ISTANBUL; Barbaros Hayrettin Naval Architecture and Maritime Faculty, Iskenderun Technical University, Iskenderun, HATAY; ORCID: 0000-0003-3523-140X

⁴Dept. of Naval Architecture and Marine Engineering, Yildiz Technical University, Besiktas, ISTANBUL; ORCID: 0000-0002-9650-3651

Received: 12.10.2019 Revised: 08.01.2020 Accepted: 21.02.2020

ABSTRACT

Internal combustion engines (ICEs) have harmful effects on the environment in terms of emissions. According to present emission regulations, reducing NO_x emissions came into prominence. One of the techniques of reducing NO_x emissions is implementation of Miller Cycle to the engine. A comparative performance analysis and optimization based on the non-dimensional power output and thermal efficiency criteria have been performed for an irreversible Dual-Miller Cycle. The effect of the design parameters such as cycle compression ratio, cut-off ratio and Miller cycle ratio of the cycle have also been investigated on the basis of having the internal irreversibility with assuming the working fluid is an ideal gas with constant specific heat. Performance analysis has been also extended to the Otto-Miller and Diesel-Miller cycles which may be considered as two special cases of the Dual-Miller cycle. The analysis and optimization study carried out in this work are hoped to provide guidelines for optimal design in terms of power output and thermal efficiency for internal combustion engines.

Keywords: Irreversible, miller cycle, performance analysis, power output, thermal efficiency.

1. INTRODUCTION

Internal combustion engines (ICEs) are very important devices used in every area of daily life and industry. ICEs have harmful effects on the environment in terms of emissions. We cannot expect the ICEs to disappear. So we should try to find ways of lowering emissions. According to present emission regulations, reducing NO_x emissions came into prominence. One of the techniques of reducing NO_x emissions is implementation of Miller Cycle to the engine. A number of recent studies have investigated the modification of existing conventional engines for operation on a Miller cycle. Mikalsen et al. compared the Miller cycle engine with a standard Otto cycle

* Corresponding Author: e-mail: yust@yildiz.edu.tr, tel: (212) 383 28 51

engine using cycle analyses and multidimensional simulation. They found that the Miller cycle engine has a potential for improved fuel efficiency, but at the cost of a reduced power to weight ratio. They suggested that there may be a fuel efficiency advantage of 5-10% compared to a standard Otto cycle engine [1].

Endo et al. described the design of a commercially available large scale gas engine using the Miller Cycle principle. They claimed that fuel efficiency advantage is possible more than 5% over conventional engine [2]. Al-Sarkhi et al. theoretically investigated the optimal power-density characteristics for Atkinson, Miller and Dual cycles without any losses [3]. Al-Sarkhi et al. also analyzed the behavior for an irreversible Miller cycle with losses arising from heat resistance and friction. They showed that there are significant effects of the temperature-dependent specific heat of the working fluid on the performance characteristics of the cycle [4]. In their other study, they used finite-time thermodynamics to derive the relations between thermal efficiency, compression and expansion ratios for an ideal naturally-aspirated (air-standard) Miller Cycle assuming that the specific heat of the working fluid varies linearly with temperature. They concluded that the effect of the temperature-dependent specific heat of the working fluid on the irreversible cycle performance is significant [5]. Ebrahimi et al. studied on the performance of an air standard irreversible Miller cycle by using finite-time thermodynamics theory. Their results show that if compression ratio exceeds certain value, the power output first increases and then starts to decrease with increasing relative air-fuel ratio, while if compression ratio exceeds certain value, the power output decreases with increasing relative air-fuel ratio. We can also see from the results that if the compression ratio is less than certain value, the power output decreases with increasing stroke length, while if compression ratio exceeds certain value, the power output first increases and then starts to decrease with increasing stroke length [6]. Also again in a different study Ebrahimi et al. shows that if the compression ratio is less than a certain value, the increase of the specific heat ratio will make the power output bigger. In contrast, if the compression ratio exceeds that certain value, the increase of the specific heat ratio will make the power output less [7]. Zhao and Chen conducted a study related to theoretical Miller cycle engine performance. They investigated the influence of the main engine design variables and system irreversibilities on Miller Cycle engine performance [8]. Gheorghiu and Ueberschär carried out a study on over expanded engine for use in hybrid vehicles and investigated sources of efficiency loss in such cycles [9]. Wang et al. investigated the feasibility of the application of the late valve closing Miller cycle concept to reduce engine exhaust gas emissions. They found that significant NO_x reductions could be achieved [10], [11]. Wang et al. investigated the application of the feasibility of applying the Miller Cycle to gasoline engines to reduce NO_x emissions. Their results showed that it was feasible to apply the Miller Cycle to gasoline engines in order to reduce NO_x emissions. In order to compensate for the charge which leads to the power losses, they also suggested carrying out an investigation on the application of a supercharger with an inter-cooler added to the Miller cycles. A better engine performance with NO_x reduction may then be able to be achieved [12]. The effects of heat loss as a percentage of fuel's energy, friction and variable specific heats of working fluid on the performance of a Miller-cycle engine under the restriction of maximum cycle temperature are presented by Lin and Hou. They concluded that these effects should be considered in practice cycle analysis [13]. Gonca et al. have studied the late inlet valve closing Miller cycle which is applied to diesel engine by lowering compression ratio with respect to expansion ratio by closing intake valve 10 and 20 crank angles later than that of standard diesel engine by using zero-dimensional single zone combustion model which was verified with experimental data. The obtained results verified with experimental data have been compared with standard diesel engine in terms of performance and NO emissions, and reported improved performance and reduction in NO emission [14]. Rinaldini et al. tried to explore potential of the Miller cycle, applied to High Speed Direct Injection (HSDI) Diesel engines [15]. According to Gonca et al. Miller Cycle study demonstrated different retarding angles with camshafts and steam injection rate on engine polluting emissions [16], [17], [18]. Gonca et al. conducted studies to

determine Miller cycled engine's performance parameters with the effects of heat transfer, emission characteristics and also the effects of turbocharge and steam injection implementation [19]–[22]. Using turbocharging compensates power loss by Miller application, and also NO, HC, CO and CO₂ emissions are reduced. In Miller cycle analysis, effect of cycle parameters, Miller cycle ratio, cycle temperature ratio, cycle pressure ratio, etc., on cycle performance are investigated. And, cycle parameters are optimized for cycle performance, power and efficiency. With steam injection, to turbocharged and Miller applied cycle provide benefit for engine performance regarding operating conditions are reported. Moreover, Miller cycle is compared with the other internal combustion engine cycles in terms of thermodynamic performance [23]. Ust et al. studied a comparative performance analysis and optimization based on exergetic performance criterion, total exergy output and exergy efficiency has been carried out for an irreversible Dual Miller Cycle cogeneration system [24].

In the present study, apart from the above studies, a comparative performance analysis and optimization based on the power output and thermal efficiency criteria has been performed for an air-standard irreversible internal combustion engine Dual-Miller cycle. The effect of the design parameters such as compression ratio, pressure ratio, cut-off ratio and Miller cycle ratio of the cycle have also been investigated on the basis of having the internal irreversibility. Performance analysis has been also extended to the Otto-Miller and Diesel-Miller cycles which may be considered as two special cases of the Dual-Miller cycle.

2. THERMODYNAMIC ANALYSIS OF DUAL-MILLER CYCLE

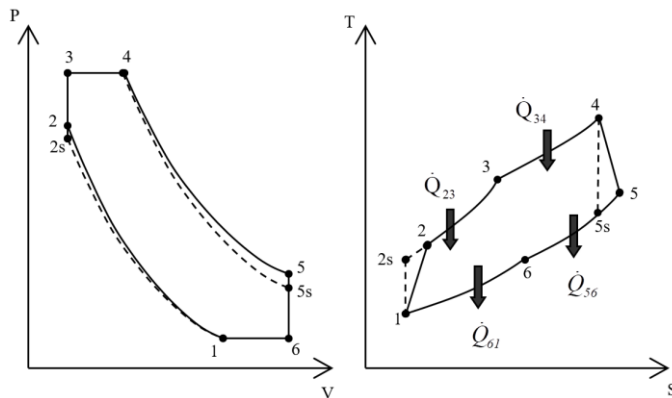


Figure 1. P-V and T-S diagrams for the Dual-Miller cycle

P-v and T-s diagrams of considered irreversible air-standard Dual-Miller cycle (1-2-3-4-5-6-1) are shown in Fig.1. In the diagrams, the process 1-2s is an isentropic compression while the process 1-2 takes into account internal irreversibilities. The heat addition occurs in two steps: processes 2-3 and 3-4 are constant volume and constant pressure heat addition processes respectively. Process 3-4 also makes up the first part of the power stroke. Process 4-5s is an isentropic expansion while the process 4-5 takes into account internal irreversibilities. The heat rejection occurs in two steps: 5-6 and 6-1 are constant volume and constant pressure heat rejection processes respectively. Assuming the working fluid is an ideal gas with constant specific heat, the rates at which heat is supplied, \dot{Q}_{in} and rejected \dot{Q}_{out} , are given by:

$$\dot{Q}_{in} = \dot{Q}_{23} + \dot{Q}_{34} = \dot{m} [C_V (T_3 - T_2) + C_P (T_4 - T_3)] \quad (1)$$

and

$$\dot{Q}_{out} = \dot{Q}_{56} + \dot{Q}_{61} = \dot{m} [C_v(T_5 - T_6) + C_p(T_6 - T_1)] \tag{2}$$

where C_v and C_p are the constant volume and constant pressure specific heat capacities and T_1, T_2, T_3, T_4, T_5 and T_6 are temperatures at states 1, 2, 3, 4, 5 and 6 respectively and \dot{m} is the mass flow rate. From the first law of thermodynamics, the power output of the cycle can be written in the form

$$\dot{W}_{DM} = \dot{Q}_{in} - \dot{Q}_{out} = \dot{m} C_v [(T_3 - T_2) + k(T_4 - T_3) - (T_5 - T_6) - k(T_6 - T_1)] \tag{3}$$

and the thermal efficiency can be written as

$$\eta_{DM} = \frac{\dot{W}_{DM}}{\dot{Q}_{in}} = 1 - \frac{\dot{Q}_{out}}{\dot{Q}_{in}} = 1 - \frac{[(T_5 - T_6) + k(T_6 - T_1)]}{[(T_3 - T_2) + k(T_4 - T_3)]} \tag{4}$$

where k is the ratio of the specific heat capacities (C_p / C_v). For the two adiabatic processes, the compression and expansion efficiencies [25]

$$\eta_C = \frac{T_{2s} - T_1}{T_2 - T_1} \tag{5}$$

and

$$\eta_E = \frac{T_4 - T_5}{T_4 - T_{5s}} \tag{6}$$

can be used to describe the irreversibility of the adiabatic processes. By using Eqs. (5) and (6), we obtain:

$$(T_2 / T_1) = \frac{\eta_C + (\varepsilon^{k-1} - 1)}{\eta_C} \tag{7}$$

and

$$(T_5 / T_4) = \{ 1 - \eta_E [1 - (1 / \delta^{k-1})] \} \tag{8}$$

where the compression ratio (ε) is given as:

$$\varepsilon = V_1 / V_2. \tag{9}$$

Let us define the principal engine design parameters such as: the pressure ratio (β), cut-off ratio (ρ) and cycle temperature ratio (α) used in the analysis are also given respectively as:

$$\beta = P_3 / P_2 = T_3 / T_2 \tag{10}$$

$$\rho = v_4 / v_3 = T_4 / T_3 \tag{11}$$

and

$$\alpha = T_{max} / T_{min} = T_4 / T_1. \tag{12}$$

In order to compare the difference between Dual-Miller cycle and Dual cycle, a concept of ‘‘Dual-Miller cycle ratio r_M ’’ is adopted to describe the difference [11]. The Miller cycle ratio is defined as:

$$r_M = v_6 / v_1 = T_6 / T_1 \tag{13}$$

when $r_M = 1$, the Dual-Miller cycle is identical with the Dual cycle. From the second law of thermodynamics, the following equation is obtained:

$$T_1^k T_3^{1-k} T_4^k = T_{2S} T_{5S} T_6^{k-1} \tag{14}$$

The relationship among $\varepsilon, \rho, \delta$ and r_M can be expressed in Eq.15, using Eqs. (5)-(13) and (14).

$$\delta = \frac{r_M \varepsilon}{\rho} \tag{15}$$

Using Eqs. (5)-(15) into the Eqs. (3) and (4) re-arranged in terms of cycle parameter, the power output and thermal efficiency can be found as follows:

$$\dot{W}_{DM} = (\dot{m} C_v T_1) \left(\frac{a_1}{\rho} + r_M (1-k) + k + \alpha \left[a_2 - \frac{\eta_E \rho^k}{(a_3 \rho + a_4)} \right] \right) \tag{16}$$

and

$$\eta_{DM} = \frac{\left(\frac{a_1}{\rho} + r_M (1-k) + k + \alpha \left[a_2 - \frac{\eta_E \rho^k}{(a_3 \rho + a_4)} \right] \right)}{(a_1 / \rho) + \alpha k} \tag{17}$$

where

$$\begin{aligned} a_1 &= \frac{\alpha [\beta (1-k) - 1]}{\beta} \\ a_2 &= k - (1 - \eta_E) \\ a_3 &= (1 - \eta_C) r_M^{k-1} \\ a_4 &= \frac{\alpha \eta_C r_M^{k-1}}{\beta} \end{aligned}$$

are defined for the sake of simplicity. The dimensionless power output ($\bar{W}_{DM} = \dot{W}_{DM} / (\dot{m} C_v T_1)$) and thermal efficiency (η_{DM}) given in Eqs. (16) and (17) can be plotted with respect to the cut-off ratio (ρ) for different values of the pressure ratio (β) and Dual-Miller cycle ratio (r_M) as shown in Figs. (2) and (3). As it can be seen from the figures, there exists a specific ρ that maximizes the \bar{W}_{DM} and η_{DM} for a given $\alpha, \beta, r_M, \eta_C$ and η_E values. Therefore, the power output given in Eq. (16) can be maximized by taking the derivative of \bar{W}_{DM} with respect to the pressure ratio (β) and cut-off ratio (ρ) as follows:

$$\frac{\partial \dot{W}_{DM}}{\partial \beta} = 0 \Rightarrow \beta_{mp} = \frac{\alpha \eta_C r_M^{k-1}}{\sqrt{\alpha \eta_C \eta_E r_M^{k-1} \rho^{(k+1)/2} - a_3 \rho}} \tag{18}$$

$$\frac{\partial \dot{W}_{DM}}{\partial \rho} = -\frac{a_1}{\rho} - \frac{\alpha \eta_E \rho^{(k-1)} [a_4 k + a_3 (k-1) \rho]}{(a_4 + a_3 \rho)^2} = 0 \tag{19}$$

It is also possible to find the optimum pressure ratio (β_{mef}) and cut-off ratio (ρ_{mef}) at maximum thermal efficiency by differentiating with respect to β and ρ and seeking a maximum thermal efficiency, $(\eta_{DM})_{max}$, by setting it equal to zero

$$\frac{\partial \eta_{DM}}{\partial \beta} = 0 \Rightarrow \beta_{mef} = \frac{\alpha \eta_C r_M^{k-1} (a_6 + a_3 a_3 \rho) + \sqrt{a_6 (\alpha \eta_C r_M^{k-1})^2 [a_6 + a_3 (a_7 + a_3 \rho)]}}{a_6 (a_7 - a_3 \rho) - a_3^2 a_3 \rho^2} \tag{20}$$

$$\frac{\partial \eta_{DM}}{\partial \rho} = \frac{\beta \left\{ a_5 [I + \beta(k - I)] - \frac{a_6 \beta (a_8 + a_9)}{a_{10}} \right\}}{a_{11}} = 0 \tag{21}$$

where

$$\begin{aligned} a_5 &= [k(\alpha + r_M - I) - (r_M + a_2 \alpha)] \\ a_6 &= \alpha \eta_E \rho^k \\ a_7 &= \alpha \eta_C r_M^{k-1} [I + k(\rho - I)] \\ a_8 &= \alpha \eta_C r_M^{k-1} [(\beta - I) + k\{\beta(\rho - I) - I\}] \\ a_9 &= a_3 k \beta \rho [\beta(k - I)(\rho - I)] \\ a_{10} &= (\alpha \eta_C r_M^{k-1} + a_3 \beta \rho)^2 \\ a_{11} &= \alpha [\beta \{I + k(\rho - I)\} - I]^2 \end{aligned}$$

are defined for the sake of simplicity. However, the equations appear to involve the variables to be solved for in an essentially non-algebraic way. Therefore, the solution procedure is carried out numerically in order to implement the theoretical proposition into practical engineering design perspectives. The relations between the power output \dot{W}_{DM} and the Miller cycle ratio r_M , as well as between the thermal efficiency η_{DM} and the Miller cycle ratio r_M , can be derived from Eqs. (16) and (17). The maximum power and the corresponding efficiency can be obtained by numerical calculations.

3. RESULTS AND DISCUSSION

To see the advantages and disadvantages of the design at maximum power output conditions (mp), detailed numerical examples are provided and compared with those of the maximum thermal efficiency (mef) for an irreversible air-standard Dual-Miller cycle. In the numerical calculations, the parameters are taken as $C_p = 1.005 \text{ kJ/kgK}$, $C_v = 0.718 \text{ kJ/kgK}$, $k = 1.4$, $\alpha = 7$ and $\eta_C = \eta_E = 0.9$. The results obtained herein include some special cases. For example:

i) When $\rho = 1$, the Dual-Miller cycle becomes a steady flow air standard Otto-Miller (OM) cycle with one constant-volume heating branch, one constant-volume and one constant-pressure cooling branches, and two adiabatic branches. Eqs. (16) and (17) become:

$$\dot{W}_{OM} = (\dot{m} C_v T_1) \left(a_1 + r_M (I - k) + k + \alpha \left[a_2 - \frac{\eta_E}{(a_3 + a_4)} \right] \right) \tag{22}$$

$$\eta_{OM} = \frac{\left(a_1 + r_M (1-k) + k + \alpha \left[a_2 - \frac{\eta_E}{(a_3 + a_4)} \right] \right)}{a_1 + \alpha k} \tag{23}$$

ii) When $\beta = 1$, the Dual-Miller cycle becomes a steady flow air standard Diesel-Miller (*DM*) cycle with one constant-pressure heating branch, one constant-volume and one constant-pressure cooling branches, and two adiabatic branches. Eqs. (16) and (17) become:

$$\dot{W}_{DM} = (\dot{m} C_v T_1) \left(\alpha (1-k/\rho) + r_M (1-k) + k + \left[a_2 - \frac{\eta_E \rho^k}{(a_3 \rho + \alpha \eta_C r_M^{(k-1)})} \right] \right) \tag{24}$$

$$\eta_{DM} = \frac{\left(\alpha (1-k/\rho) + r_M (1-k) + k + \left[a_2 - \frac{\eta_E \rho^k}{(a_3 \rho + \alpha \eta_C r_M^{(k-1)})} \right] \right)}{\alpha k (1-1/\rho)} \tag{25}$$

There are also some other special cases, for example when $r_M = 1$ and $\rho = 1$ the cycle becomes Otto cycle and when $r_M = 1$ and $\beta = 1$ the cycle becomes Diesel cycle.

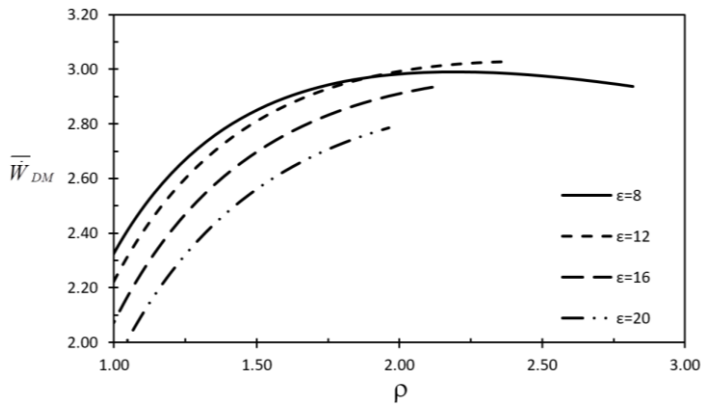


Figure 2(a). Non-dimensional power output vs cut-off ratio for different values of the compression ratio with $r_M=1.5$

Using Eqs. (16) and (17) together with the second law constraint given in Eq. (14), the variation of dimensionless power output (\bar{W}_{DM}) and thermal efficiency (η_{DM}) with respect to the cut-off ratio (ρ) for different values of ϵ and r_M are presented in Fig.2-3. By observing Fig. 2-3, one can see that the maximum power output, $(\bar{W}_{DM})_{max}$ condition and also corresponding optimal cut-off ratios (ρ_{mp}, ρ_{mef}) decrease for increasing ϵ values. However, in contrast maximum thermal efficiency, $(\eta_{DM})_{max}$ increase for increasing ϵ values. It is also observed that as r_M increases, $(\bar{W}_{DM})_{max}$ and $(\eta_{DM})_{max}$ increases up to a certain value and then starts decreasing. In Fig. 2a and 2b. Fig. 2a demonstrates power output decreases with the increase of

compression ratio. On the other hand, it can be seen from Fig. 2b thermal efficiency increases with the increase of compression ratio.

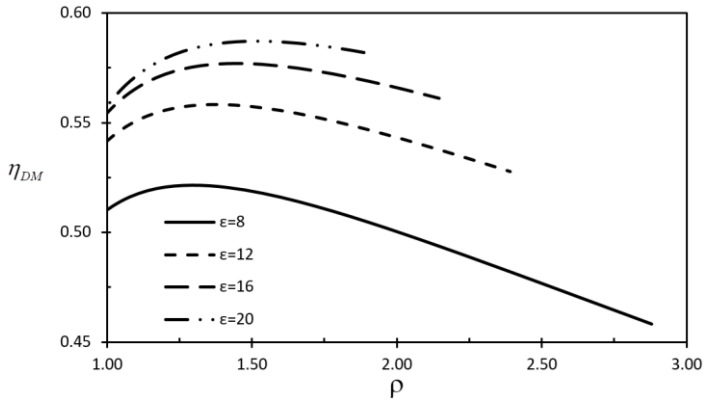


Figure 2(b). Thermal efficiency vs cut-off ratio for different values of the compression ratio with $r_M=1.5$

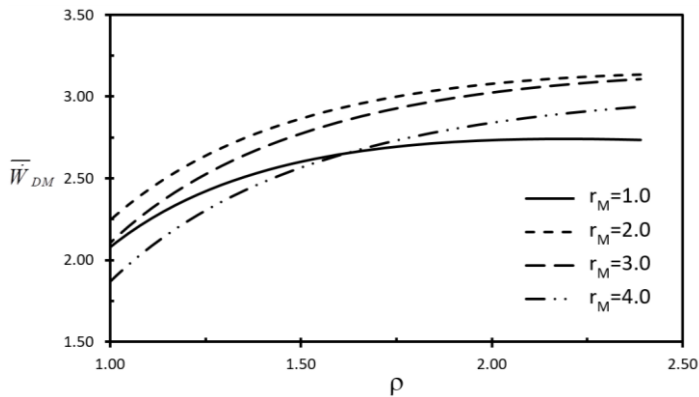


Figure 3(a). Non-dimensional power output vs cut-off ratio for different values of the Miller cycle ratio with $\epsilon=12$

The variation of dimensionless power output (\bar{W}_{DM}) and thermal efficiency (η_{DM}) with respect to the cut-off ratio (ρ) for different values of r_M are given in Fig. 3a and 3b. Fig. 3a demonstrates power output decreases with the increase of Miller cycle ratio after $r_M=2$ value. According to analysis, maximum power output is seen at $r_M=2.47$ value. Similarly it can be seen from Fig. 3b thermal efficiency decreases with the increase of Miller cycle ratio after $r_M=2$ value. Maximum thermal efficiency is seen at $r_M=2.05$ value according to analysis. In Fig. 4, the variation of the non-dimensional power output with respect to the thermal efficiency for various ϵ and r_M values are shown for Dual-Miller cycle. From Fig. 4a and b, we see that the loop curves become bigger as ϵ increase. Also, it can be observed from Fig. 4 that both \bar{W}_{DM} and

η_{DM} have separate maximums and these maximum performances in terms of \bar{W}_{DM} increase up to a certain value and then start decreasing for increasing ε values, however η_{DM} continuously increase for increasing ε values. The loop curves also move forward and up as the Miller cycle ratio, r_M increases; however the loop curves return back at some point, meaning there is an optimum condition of \bar{W}_{DM} for a certain r_M value (Fig. 4b).

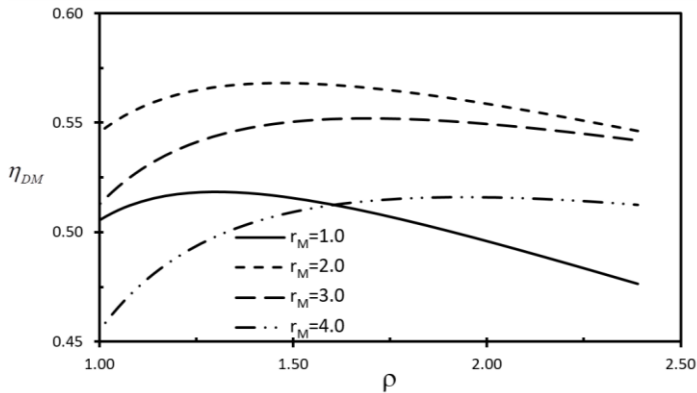


Figure 3(b). Thermal efficiency vs cut-off ratio for different values of the Miller cycle ratio with $\varepsilon=12$

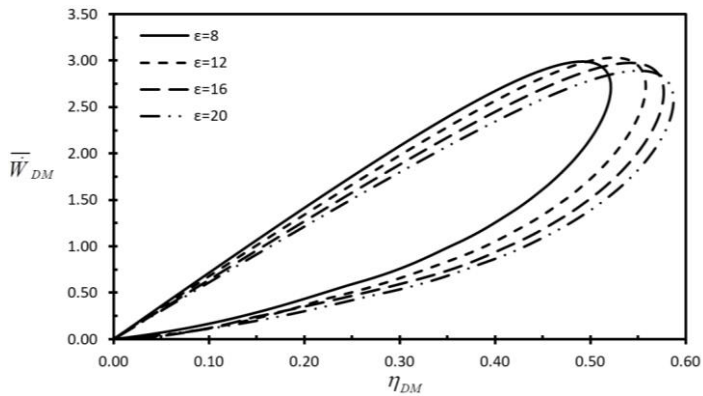


Figure 4(a). Non-dimensional power output vs thermal efficiency for different values of the compression ratio

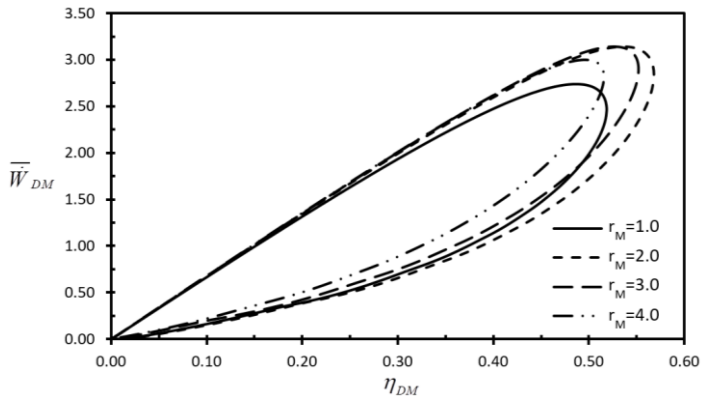


Figure 4(b). Non-dimensional power output vs thermal efficiency for different values of the Miller cycle ratio

The variations of the non-dimensional power output versus thermal efficiency are shown for Dual-Miller, Diesel-Miller and Otto-Miller cycle in Fig. 5. It is seen from Fig. 5 that the power output and thermal efficiency conditions for the Diesel-Miller cycle is always greater than Dual-Miller and Otto-Miller cycles, so we can write:

$$(\bar{W}_{dM})_{max} > (\bar{W}_{DM})_{max} > (\bar{W}_{OM})_{max} \tag{26}$$

$$(\eta_{dM})_{max} > (\eta_{DM})_{max} > (\eta_{OM})_{max} . \tag{27}$$

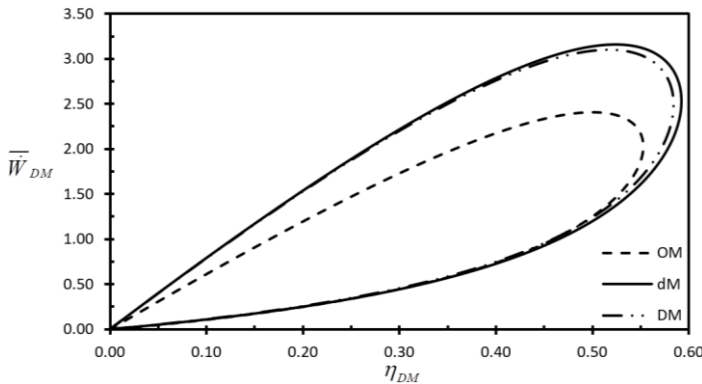


Figure 5. A comparative non-dimensional power output vs thermal efficiency graphics for the Dual-Miller, Diesel-Miller and Otto-Miller cycles

The effect of r_M on the maximum power output, thermal efficiency and corresponding optimal cut-off ratios for different ε values are shown in Fig. 6 for Dual-Miller cycle. As can be seen from the Fig. 6, when r_M increases, $(\bar{W}_{DM})_{max}$ and $(\eta_{DM})_{max}$ increase to its peak value, i.e. a ‘double-maximum’ dimensionless power output $(\bar{W}_{DM})_{max,2}$ and thermal efficiency $(\eta_{DM})_{max,2}$,

then decrease smoothly. Double-maximum term represents the optimum regarding power output and efficiency, both.

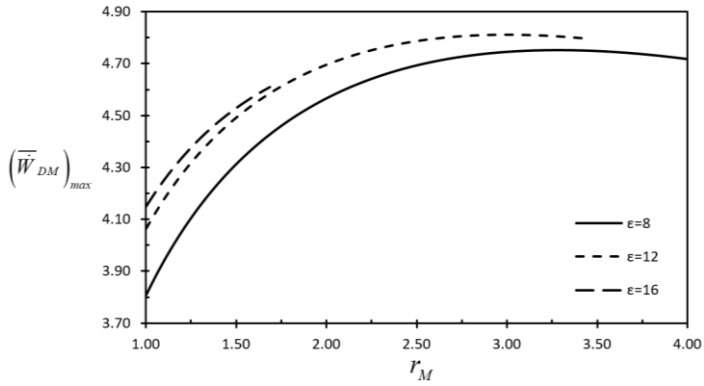


Figure 6(a). The maximum non-dimensional power output with $\alpha = 9$ vs Miller cycle ratio for different values of the compression ratio

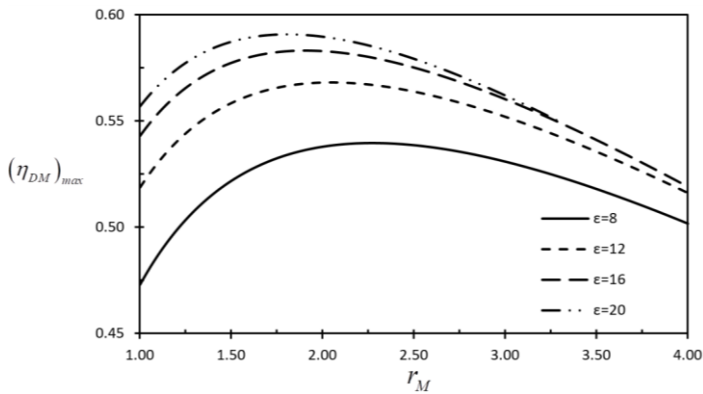


Figure 6(b). Thermal efficiency vs Miller cycle ratio for different values of the compression ratio

The effect of r_M on the corresponding optimal cut-off ratios for different ϵ values are shown in Fig. 7 for Dual-Miller cycle. It can be seen from the Fig. 7, the optimal ρ values (ρ_{mp}, ρ_{mef}) increase smoothly for increasing r_M values. The increase in compression ratio leads to increase in the cut-off ratio at maximum power output condition (ρ_{mp}) and the cut-off ratio at maximum efficiency condition (ρ_{mef}).

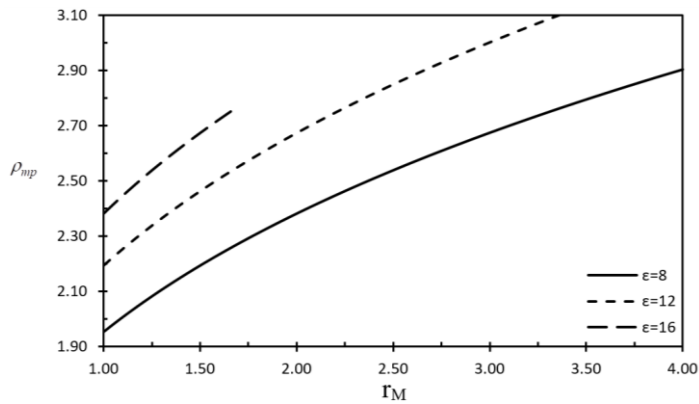


Figure 7(a). The optimal cut-off ratio at maximum power output conditions (with $\alpha = 9$) vs Miller cycle ratio for different values of the compression ratio

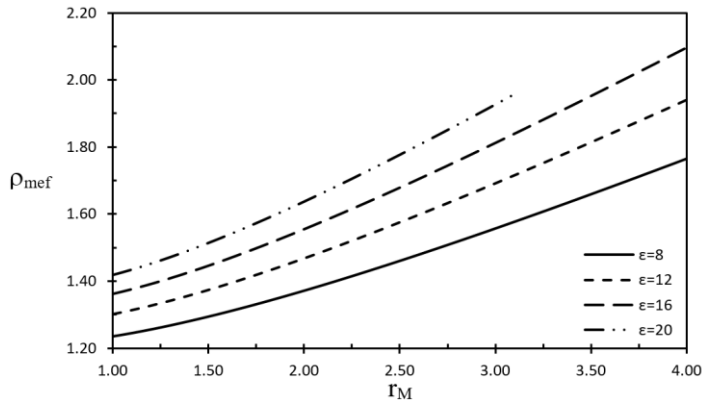


Figure 7(b). The optimal cut-off ratio at maximum thermal efficiency conditions vs Miller cycle ratio for different values of the compression ratio

4. CONCLUSION

We have presented a thermodynamic optimization to determine the optimal operation and design parameters for the irreversible air-standard Dual-Miller cycle. In this perspective, the optimum compression ratio (ϵ), cut-off ratio (ρ) and Miller cycle ratio (r_M) that maximize the power output and thermal efficiency have been investigated. The performance of the Dual-Miller cycle under maximum power output objective function is discussed and compared with respect to maximum thermal efficiency conditions. It is determined that there is a specific value of Miller cycle ratio at maximum dimensionless power output. An increase or a decrease of this specific value decreases dimensionless power output. In the same operating condition, it is determined that a different optimal value of Miller cycle ratio for maximum thermal efficiency. Otherwise power output increases to a certain value with the increase of compression ratio and then it starts to decrease. But with the increase of compression ratio, thermal efficiency increases consistently. It is observed that, there exists an optimal value for Miller cycle ratio that leads to a ‘double-maximum’ power output and thermal efficiency objectives. It is also shown that the power output

and thermal efficiency conditions for the Dual -Miller cycle is always greater than the Otto-Miller cycles corresponding the same cycle pressure ratio. However, the Dual -Miller cycle power output and thermal efficiency are very close to the Diesel-Miller cycle. Diesel-Miller cycle is presented for the operating limits. In maximum power output (mp) and maximum thermal efficiency conditions (mef), the effects of compression ratio to cut-off ratio for different Miller-cycle ratio values are demonstrated. The analysis and optimization study carried out in this work are hoped to provide guidelines for optimal design in terms of power output and thermal efficiency for internal combustion engines.

Acknowledgment

We would like to thank Turkish Academy of Sciences (TUBA-GEBIP) and The Scientific and Technological Research Council Of Turkey (TUBITAK).

NOMENCLATURE

C_p = Specific heat at constant pressure ($kJ / kg.K$)

C_v = Specific heat at constant volume ($kJ / kg.K$)

k = Isentropic exponent

\dot{m} = Mass flow rate (kg / s)

\dot{Q} = Rate of heat transfer (kW)

P = Pressure (kPa)

r_M = Miller cycle ratio

s = Entropy ($kJ / kg.K$)

T = Temperature (K)

v = Specific volume (m^3 / kg)

V = Volume (m^3)

\dot{W} = Power output (kW)

GREEK LETTERS

α = Cycle temperature ratio, $\alpha = T_{max} / T_{min} = T_4 / T_1$

β = Pressure ratio, $\beta = p_3 / p_2 = T_3 / T_2$

ε = Compression ratio, $\varepsilon = V_1 / V_2$

δ = Expansion ratio, $\delta = V_5 / V_4$

∂ = Derivative

η = Thermal efficiency

η_c = Isentropic efficiency of compression

η_e = Isentropic efficiency of expansion

ρ = Cut-off ratio, $\rho = v_4 / v_3 = T_4 / T_3$

Subscripts

dM = Diesel-Miller

DM = Dual-Miller

in = input

max = Maximum

mef = at maximum thermal efficiency condition

min = Minimum

mp = at maximum power output condition

OM = Otto-Miller

out = output

Superscripts

— = non-dimensional

REFERENCES

- [1] R. Mikalsen, Y. D. Wang, and A. P. Roskilly, "A comparison of Miller and Otto cycle natural gas engines for small scale CHP applications," *Applied Energy*, vol. 86, no. 6, pp. 922–927, Jun. 2009.
- [2] H. Endo, K. Tanaka, Y. Kakuhamu, Y. Goda, T. Fujiwaka, and M. Nishigaki, "Development of the lean burn Miller cycle gas engine," *The Fifth International on Diagnostics and Modeling of Combustion in Internal Combustion Engines–COMODIA 2001*, pp. 374–380, 2001.
- [3] A. Al-Sarkhi, B. A. Akash, J. O. Jaber, M. S. Mohsen, and E. Abu-Nada, "EFFICIENCY OF MILLER ENGINE AT MAXIMUM POWER DENSITY," *International Communications in Heat and Mass Transfer*, vol. 29, no. 8, pp. 1159–1167, Nov. 2002.
- [4] A. Al-Sarkhi, J. O. Jaber, and S. D. Probert, "Efficiency of a Miller engine," *Applied Energy*, vol. 83, no. 4, pp. 343–351, Apr. 2006.
- [5] A. Al-Sarkhi, I. Al-Hinti, E. Abu-Nada, and B. Akash, "Performance evaluation of irreversible Miller engine under various specific heat models," *International Communications in Heat and Mass Transfer*, vol. 34, no. 7, pp. 897–906, Aug. 2007.
- [6] R. Ebrahimi, "Performance analysis of an irreversible Miller cycle with considerations of relative air–fuel ratio and stroke length," *Applied Mathematical Modelling*, vol. 36, no. 9, pp. 4073–4079, Sep. 2012.
- [7] R. Ebrahimi, "Thermodynamic modeling of performance of a Miller cycle with engine speed and variable specific heat ratio of working fluid," *Computers & Mathematics with Applications*, vol. 62, no. 5, pp. 2169–2176, Sep. 2011.
- [8] Y. Zhao and J. Chen, "Performance analysis of an irreversible Miller heat engine and its optimum criteria," *Applied Thermal Engineering*, vol. 27, no. 11–12, pp. 2051–2058, Aug. 2007.
- [9] V. Gheorghiu and D. Ueberschär, "Enhancement potential of the thermal conversion efficiency of ICE cycles especially for use in hybrid vehicles," in *5th Int. Conference on Heat Transfer, Fluid Mechanics and Thermodynamics (HEFEAT2007)*, Sun City, South Africa, 2007.
- [10] Y. Wang and T. Ruxton, "An experimental investigation of NO_x emission reduction from automotive engine using the Miller cycle," in *ASME 2004 Internal Combustion Engine Division Fall Technical Conference*, 2004, pp. 181–189.

- [11] Y. Wang *et al.*, “An analytic study of applying Miller cycle to reduce NO_x emission from petrol engine,” *Applied Thermal Engineering*, vol. 27, no. 11–12, pp. 1779–1789, Aug. 2007.
- [12] Y. Wang *et al.*, “Application of the Miller cycle to reduce NO_x emissions from petrol engines,” *Applied Energy*, vol. 85, no. 6, pp. 463–474, Jun. 2008.
- [13] J.-C. Lin and S.-S. Hou, “Performance analysis of an air-standard Miller cycle with considerations of heat loss as a percentage of fuel’s energy, friction and variable specific heats of working fluid,” *International Journal of Thermal Sciences*, vol. 47, no. 2, pp. 182–191, 2008.
- [14] G. Gonca, B. Sahin, Y. Ust, and A. Parlak, “A study on late intake valve closing miller cycled diesel engine,” *Arabian Journal for Science and Engineering*, vol. 38, no. 2, pp. 383–393, 2013.
- [15] C. A. Rinaldini, E. Mattarelli, and V. I. Golovitchev, “Potential of the Miller cycle on a HSDI diesel automotive engine,” *Applied Energy*, vol. 112, pp. 102–119, 2013.
- [16] G. Gonca *et al.*, “The effects of steam injection on the performance and emission parameters of a Miller cycle diesel engine,” *Energy*, vol. 78, pp. 266–275, 2014.
- [17] G. Gonca *et al.*, “Theoretical and experimental investigation of the Miller cycle diesel engine in terms of performance and emission parameters,” *Applied Energy*, vol. 138, pp. 11–20, 2015.
- [18] G. Gonca, B. Sahin, Y. Ust, A. Parlak, and A. Safa, “Comparison of steam injected diesel engine and miller cycled diesel engine by using two zone combustion model,” *Journal of the Energy Institute*, vol. 88, no. 1, pp. 43–52, 2015.
- [19] G. Gonca, B. Sahin, A. Parlak, V. Ayhan, İ. Cesur, and S. Koksall, “Application of the Miller cycle and turbo charging into a diesel engine to improve performance and decrease NO emissions,” *Energy*, vol. 93, pp. 795–800, Dec. 2015.
- [20] G. Gonca, B. Sahin, and Y. Ust, “Investigation of Heat Transfer Influences on Performance of Air-Standard Irreversible Dual-Miller Cycle,” *Journal of Thermophysics and Heat Transfer*, vol. 29, no. 4, pp. 678–683, Oct. 2015.
- [21] G. Gonca, B. Sahin, and Y. Ust, “Performance maps for an air-standard irreversible Dual-Miller cycle (DMC) with late inlet valve closing (LIVC) version,” *Energy*, vol. 54, pp. 285–290, Jun. 2013.
- [22] G. Gonca and B. Sahin, “The influences of the engine design and operating parameters on the performance of a turbocharged and steam injected diesel engine running with the Miller cycle,” *Applied Mathematical Modelling*, vol. 40, no. 5–6, pp. 3764–3782, Mar. 2016.
- [23] G. Gonca, “Comparative performance analyses of irreversible OMCE (Otto Miller cycle engine)-DiMCE (Diesel miller cycle engine)-DMCE (Dual Miller cycle engine),” *Energy*, vol. 109, pp. 152–159, Aug. 2016.
- [24] Y. Ust, F. Arslan, I. Ozsari, and M. Cakir, “Thermodynamic performance analysis and optimization of DMC (Dual Miller Cycle) cogeneration system by considering exergetic performance coefficient and total exergy output criteria,” *Energy*, vol. 90, pp. 552–559, 2015.
- [25] L. Chen, C. Wu, and F. Sun, “Finite time thermodynamic optimization or entropy generation minimization of energy systems,” *Journal of Non-Equilibrium Thermodynamics*, vol. 24, no. 4, pp. 327–359, 1999.